

Enhancing Transmission over Wireless Image Sensor Networks Based on ZigBee Network

Ahmed A. Abouelfadl¹, M. A. M. El-Bendary² and F. Shawki¹

¹ Department of Electrical Engineering, Faculty of Engineering, Rabigh 21911, King Abdulaziz University, Saudi Arabia

¹ Department of Electronics and Electrical Communications, Faculty of Electronic Engineering, Menoufia University, Menouf, 32952, Egypt.

² Department of Communication Technology, Faculty of Industrial Education, Helwan University, Egypt
E-mails: ahmed251056@yahoo.com, mohsenbendary@hotmail.com, farid_shawki@yahoo.com.

Abstract: Different scenarios for the efficient transmission of images over wireless sensor networks are presented. The research is focused on the use of the IEEE 802.15.4 ZigBee for applying the proposed scenarios. The heart of these scenarios is a novel chaotic interleaving scheme, which can tolerate error bursts. The investigation studies the performance of the proposed interleaver with convolutional codes having different constraint lengths (K). A comparison study between the traditional block interleaving scheme and the proposed chaotic interleaving scheme for image transmission over a correlated fading channel is presented. The simulation results show the superiority of the proposed chaotic interleaving scheme. The results also prove that the chaotic interleaver on a packet-by-packet basis gives a high quality image with (K=3) and eliminates the need for a complex encoder having K=7.

[Ahmed A. Abouelfadl, M. A. M. El-Bendary and F. Shawki. **Enhancing** Transmission over Wireless Image Sensor Networks Based on ZigBee Network. *Life Sci J* 2014;11(8):342-354]. (ISSN:1097-8135). <http://www.lifesciencesite.com>. 46

Keywords: Wireless Image Sensor networks, ZigBee, interleaving technique chaotic based, convolutional coding.

1. Introduction

With widely utilization of the Wireless Sensors Networks (WSN) and its variety applications, there are two important factors that deserve consideration; power efficiency and throughput. The paper concerns on these two factors, the reduction of consumed power is the vital point in WSN applications. The second factor is the throughput, it measures the success degree of the sensing node in transferring the monitored event or phenomena, low throughput means unreliable link also, the WSN purpose fail. The behavior of the WSN communications channel is wireless channel, there are high probability of packet loss. The lost packets can not be compensated, where it contacts to the real-time world. The different error control schemes are used to Limits effect of transmission process and reduces errors contained occur [1-2].

In wireless sensor networks (WSNs) an important trade-off exists between transmission continuity and resilience and energy-efficiency. The spread-spectrum techniques utilized in the most prevalent wireless sensor network standard, IEEE 802.15.4, provides high reliability in high interference environments. However, in many situations it may provide far higher Signal to Noise Ratio (SNR) than required and therefore waste energy by unnecessarily reducing throughput [3].

It is known that the WSN channel is wireless radio channel is time varying and can have high bit error rates. In order to improve the reliability of the

data sent in the wireless channel, some techniques can be employed, such as automatic repeat request (ARQ) and forward error correction (FEC). Although an error control strategy improves the reliability of a packet, the energy consumed due to the transmission of the additional bits in these coded schemes contributes to increase the energy consumption. The paper presents the way to enhance the performance of WSN with the interleaving technique chaotic based with additional security enhancing [4].

Over bad communication channels, different Forward Error Correction (FEC) schemes are used [5]. In this paper, the convolutional coding is used as an FEC technique, because it can significantly improve the performance of communication systems. The Viterbi algorithm is one of the most widely used decoding algorithms for convolutional codes. It is optimal, but its complexity in both the number of computations and memory requirements is exponentially increased with the constraint length K of the code. So, practically, the constraint length K of convolutional codes is limited to $K < 9$. Hence, when codes with longer constraint lengths are required in order to achieve a lower error probability, decoding algorithms whose complexity does not depend on the constraint length become especially attractive [6-7].

In fact, the environment of mobile communications suffers from long burst errors. In the fast fading case, these burst errors are due to the multipath effect, and they reduce the quality of communication. An error control technique in mobile

communication is not enough with long burst errors [8]. In [9], the effect of interleaved convolutional coding with code rate 1/2 and $K=7$ on image transmission over a wireless channel was studied. The adaptive Viterbi decoding for interleaved convolutional coding was presented in [10] and [11], but with little improvement. In fact, there is a need for an effective error spreading tool to enhance the quality of communication.

This paper presents a novel technique to achieve a lower error probability with a small constraint length of the convolutional encoder. This technique depends on the data interleaving or randomization. So, long burst errors can be separated into single random or short burst errors. Computer simulations have been carried out on the proposed chaotic interleaver for the ZigBee network assuming the Jakes channel model. The simulation results have revealed that the proposed technique is efficient for image communication over the ZigBee network [12].

The paper is organized as follows. The brief of WSN concepts is presented in section 2. In section 3, a review on the ZigBee standard is introduced. In section 4, the proposed modifications are presented. In section 5, the simulation assumptions and the simulation results are presented. Finally, the conclusion is presented in section 6.

2. WSN Concepts

It is good and practically to find a wireless network has arm to sense the surround events and own eyes to see the changes and monitoring the objects, it is the wireless sensor network. A WSN can be defined as a wireless network has group of devices, denoted as Sensing Nodes (SN), which can sense and monitor the environment and communicate the information gathered from the monitored field [13-14]. The data is forwarded, possibly via multiple hops, to a sink (sometimes denoted as controller or monitor) that can use it locally or is connected to other networks (the Internet for example) through a gateway. The nodes can be stationary or moving. They can be aware of their location or not. They can be homogeneous or not.

The variety of possible applications of WSNs to the real world is practically unlimited, from environmental monitoring [15], health care [16], positioning and tracking [17], to logistic, localization, and so on. Due to the wide variety of possible applications of WSNs, system requirements could change significantly.

For instance, in case of environmental monitoring applications, the following requirements are typically dominant: energy efficiency, nodes are battery powered or have a limited power supply; low data rate, typically the amount of data to be sensed is

limited; one-way communication, nodes act only as sensors and hence the data flow is from nodes to sink(s); wireless backbone, usually in environmental monitoring no wired connections are available to connect sink(s) to the fixed network. Significantly different are the requirements of a typical industrial application where wireless nodes are used for cable replacement: reliability, communication must be robust to failure and interference; security, communication must be robust to intentional attacks; inter-operability, standards are required; high data rate, the process to be monitored usually carries a large amount of data; two-way communication, in industrial applications nodes typically act also as actuators and hence the communication between sink(s) and nodes must be guaranteed; wired backbone, sinks can be connected directly to the fixed network using wired connections.

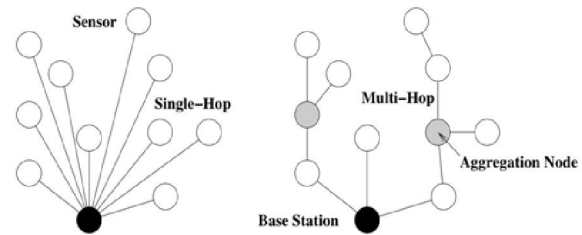


Figure 1. Single-hop versus multi-hop communication in sensor networks.

Specifically, the design of energy efficient communication protocols is a very peculiar issue of WSNs, without significant precedent in wireless network history. Generally, when a node is in transmit mode, the transceiver drains much more current from the battery than the microprocessor in active state or the sensors and the memory chip. The ratio between the energy needed for transmitting and for processing a bit of information is usually assumed to be much larger than one (more than one hundred or one thousand in most commercial platforms). For this reason, the communication protocols need to be designed according to paradigms of energy efficiency, while this constraint is less restrictive for processing tasks. Then, the design of energy efficient communication protocols is a very peculiar issue of WSNs, without significant precedent in wireless network history. Most of the literature on WSNs deals with the design of energy efficient protocols, neglecting the role of the energy consumed when processing data inside the node, and conclude that the transceiver is the part responsible for the consumption of most energy. On the other hand, data processing in WSNs may require consuming tasks to be performed at the microprocessor, much longer

than the actual length of time a transceiver spends in transmit mode. This can cause significant energy consumption by the microprocessor, even comparable to the energy consumed during transmission, or reception, by the transceiver [18].

The WSN like any wireless network to improve the reliability of the data sent in the wireless channel, techniques such as automatic repeat request (ARQ) and forward error correction (FEC) can be employed [19]. FEC employs error correcting codes to combat bit errors by adding redundancy (parity bits) to information packets. The receiver uses the parity bits to detect and correct errors. FEC techniques are associated with unnecessary overhead that increases energy consumption when the channel is relatively error free. In this work, there are some points have been covered. First point, the reliable wireless link through the WSN and the security also are focused on the presented scenarios. The second point, the complexity due to the length of processed data within the sensing node is considered in the presented simple analysis. The work within the paper is based on the interleaving technique chaotic based. This technique presents two features, powerful data randomizing tool and additional level of security for the data transmission link [20].

3. ZigBee Standard

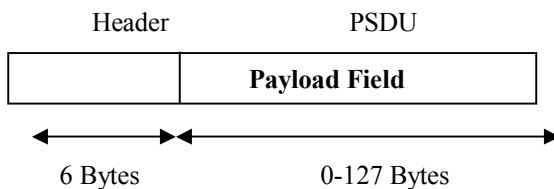


Figure 2. ZigBee packet format.

The short-range wireless networks such as the Bluetooth and ZigBee are widely used in essential applications such as health care, medical applications, home automation, and environmental applications [21-22]. The ZigBee network is a Low-Rate WPAN (LR-WPAN) that is used for short-range, low-power, and low-cost data communication. The structure of the ZigBee packet is shown in Figure 2. The header contains three fields; a preamble of 32 bits for synchronization, a packet delimiter of 8 bits, and a physical header of 8 bits. The Physical Service Data Unit (PSDU) field contains a payload of 0 to 127 bytes length. The ZigBee network uses an error detection/retransmission technique. To ensure successful reception of data, an acknowledged frame delivery protocol is supported to increase transfer reliability [23].

Table 1. IEEE 802.15.4 frequency bands and data rates.

PHY (MHz)	Freq. Band (MHz)	Mod.	Channels	Bit Rate (kbps)
868/915	868-868.6	BPSK	1	20
	902-928	BPSK	10	40
2450	2400-2483.5	O-QPSK	16	250

Low-power consumption in ZigBee networks can be achieved by allowing a device to sleep, which means waking into active mode for brief periods. Enabling such low-duty-cycle operation is at the heart of the ZigBee standard. ZigBee is built on top of the IEEE 802.15.4 standard. It offers the additional functionality to implement mesh networking rather than point-to-point networking found in most Bluetooth and Wi-Fi applications. The ZigBee specification document is short, allowing a small and simple stack, in contrast to the other wireless standards such as Bluetooth [24].

The IEEE 802.15.4 standard is intended to conform to established regulations in Europe, Japan, Canada, and the United States. It defines two physical (PHY) layers; the 2.4 GHz and 868/915 MHz band PHY layers. Although the PHY layer chosen depends on local regulations and user preference, only the higher data rate, worldwide, unlicensed 2.4 GHz Industrial, Scientific, and Medical (ISM) frequency band is considered. A group of 16 channels is available in the 2.4 GHz band, numbered from 11 to 26, each with a bandwidth of 2 MHz, and a channel separation of 5 MHz. The channel mapping frequencies are given in Table I. The LR-WPAN output powers are around 0 dBm. It typically operates within a 50-m range. The transmit scheme used is the Direct Sequence Spread Spectrum (DSSS) [25-26].

4. Proposed Modifications

The transmission of multimedia over unreliable data links has become a topic of paramount importance. This type of transmission must reconcile the high data rates involved in multimedia contents and the noisy nature of the channels, be it wireless or mobile. In this paper, there are different proposed scenarios to improve the transmission of images over the ZigBee network through interleaving. We study the feasibility of data interleaving prior to transmission over ZigBee networks. The paper presents a new chaotic interleaver and compares it to the traditional block and convolutional interleavers.

In a general convolutional code, the input information sequence contains $k \times L$ bits, where k is the number of parallel information bits at a time interval, and L is the number of time intervals. This

results in $m + L$ stages in the Trellis diagram, where m is the number of shift registers in the encoder and $K = m + 1$. There are exactly $2^k \times L$ distinct paths in the Trellis diagram. As a result, the Maximum-Likelihood (ML) sequence would have a computational complexity of $O(2^k \times L)$. The Viterbi algorithm reduces complexity by performing the ML search on a stage at a time in the Trellis diagram at each node. The number of nodes per stage in the Trellis diagram is 2^m . Therefore, the complexity of Viterbi calculations is of $O(2^k)(2^m)(m + L)$ [16]. This significantly reduces the number of calculations required to implement the ML decoding, because the number of time intervals L is now smaller [27,28]. With the increase in m and k , the complexity is increased exponentially. So, the paper tries to reduce the computational complexity through the proposed chaotic interleaver by eliminating the need of convolutional codes with large constraint lengths.

The computer simulations are based on binary non-recursive convolutional coding. The convolutional encoder uses a constituent encoder with $K=3, 5, \text{ or } 7$, code rate = $1/2$ and generator polynomials, $G = (5,7), (23,35), \text{ or } (133,171)$ in octal [28]. The paper uses the proposed chaotic interleaving technique to improve the capabilities of the convolutional codes with short constraint lengths.

4.1 Block Interleaving Scheme

The block interleaving can be used for image transmission with the ZigBee network. After converting the image into a binary sequence, this sequence is rearranged into a matrix in a row-by-row manner, and then read from the matrix in a column-by-column manner. Now take a look at how the block interleaving mechanism can correct error bursts. Assume an error burst affecting four consecutive bits (1-D error burst) as shown in Figure 2 (b) with shades. After de-interleaving as shown in Figure 2 (c), the error burst is effectively spread among four different rows, resulting in a small effect for the 1-D error burst. With a single-error correction capability, it is obvious that no decoding error will result from the presence of such 1-D error burst. This simple example demonstrates the effectiveness of the block interleaving mechanism in combating 1-D error bursts. Let us examine the performance of the block interleaving mechanism, when a 2-D (2×2) error burst occurs [29], as shown in Figure 3 (b) with shades. Figure 3 (c) indicates that the 2×2 error burst has not been spread, effectively, so that there are adjacent bits in error in the first and second rows.

As a result, this error burst can not be corrected using a single-error correction mechanism. That is, the block interleaving mechanism can not combat the 2×2 error bursts [30].

4.2 Convolutional Interleaving Scheme

The convolutional interleaver is constructed by T parallel branches. Each line contains a shift register with a predefined length [31]. The input data is fed into the branches of the interleaver and the output data is taken from the outputs of these branches. In the computer simulations, the length of the interleaver input is 1024 bits, which is the length of the whole payload in ZigBee packets [32]. The output of the convolutional interleaver with the same input stream is shown in Figure 4. As shown in the result, this interleaver performs better than the traditional block interleaver in the burst spreading but with the limited distance between the adjacent error spreading. In the case of one dimensional error, it performs worse than the block interleaver. With the two dimensional burst error case, it performs better than block interleaver as shown in Figure 5(c).

4.3 Chaotic Interleaving Scheme

The chaotic interleaver idea is presented using the logistic map in [33, 44]. This map is defined as a typical example of a 1-D chaotic map. In [33], it is applied with the turbo code. In [34], a logistic interleaver is employed in a Bit-Interleaved Coded Modulation (BICM) technique. In this work, the proposed chaotic interleaver is based on a 2-D Baker map, which is a powerful data randomization tool. This map is widely used as an encryption tool [35, 36], and it will be developed in this paper as an interleaving tool.

From Figure 3, it is clear that the block interleaver is not efficient with 2-D error bursts. As a result, there is a need for an advanced interleaver for this task. The 2-D chaotic Baker map in its discretized version is a good candidate for this purpose. After rearrangement of bits into a 2-D format, the chaotic Baker map is used to randomize the bits. Let $B(n_1, \dots, n_k)$, denote the discretized map, where the vector, $[n_1, \dots, n_k]$, represents the secret key, S_{key} . Defining N as the number of data items in one row, the secret key is chosen such that each integer n_i divides N , and $n_1 + \dots + n_k = N$.

Let $N_i = n_1 + \dots + n_{i-1}$. The data item at the indices (r, s) , is moved to the indices [37-40]:

$$B(r,s) = \left[\frac{N}{n_i} (r - N_i) + s \bmod \left(\frac{N}{n_i} \right); \frac{n_i}{N} \left(s - s \bmod \left(\frac{N}{n_i} \right) \right) + N_i \right] \quad (1)$$

where $N_i \leq r < N_i + n_i$, $0 \leq s < N$, and $N_i = 0$.

In steps, the chaotic permutation is performed as follows:

1- An $N \times N$ square matrix is divided into N rectangles of width n_i and number of elements N .

2- The elements in each rectangle are rearranged to a row in the permuted rectangle. Rectangles are taken from left to right beginning with lower rectangles then upper ones.

3- Inside each rectangle, the scan begins from the bottom left corner towards upper elements.

Figure 4 shows an example for chaotic interleaving of an 8×8 square matrix (i.e. $N = 8$). The secret key, $S_{key} = [n_1, n_2, n_3] = [2, 4, 2]$. Note that the chaotic interleaving mechanism has a better treatment to both 1-D and 2-D error bursts than the block interleaving mechanism. Errors are better distributed to bits after de-interleaving in the proposed chaotic interleaving scheme. As a result, a higher Peak Signal-to-Noise Ratio (PSNR) of received images can be achieved with this proposed mechanism. Moreover, it adds a degree of security to the communication system. At the receiver of the ZigBee system, a chaotic de-interleaving step is performed.

b_1	b_2	b_3	b_4	b_5	b_6	b_7	b_8
b_9	b_{10}	b_{11}	b_{12}	b_{13}	b_{14}	b_{15}	b_{16}
b_{17}	b_{18}	b_{19}	b_{20}	b_{21}	b_{22}	b_{23}	b_{24}
b_{25}	b_{26}	b_{27}	b_{28}	b_{29}	b_{30}	b_{31}	b_{32}
b_{33}	b_{34}	b_{35}	b_{36}	b_{37}	b_{38}	b_{39}	b_{40}
b_{41}	b_{42}	b_{43}	b_{44}	b_{45}	b_{46}	b_{47}	b_{48}
b_{49}	b_{50}	b_{51}	b_{52}	b_{53}	b_{54}	b_{55}	b_{56}
b_{57}	b_{58}	b_{59}	b_{60}	b_{61}	b_{62}	b_{63}	b_{64}

(a)

b_1	b_9	b_{17}	b_{25}	b_{33}	b_{41}	b_{49}	b_{57}
b_2	b_{10}	b_{18}	b_{26}	b_{34}	b_{42}	b_{50}	b_{58}
b_3	b_{11}	b_{19}	b_{27}	b_{35}	b_{43}	b_{51}	b_{59}
b_4	b_{12}	b_{20}	b_{28}	b_{36}	b_{44}	b_{52}	b_{60}
b_5	b_{13}	b_{21}	b_{29}	b_{37}	b_{45}	b_{53}	b_{61}
b_6	b_{14}	b_{22}	b_{30}	b_{38}	b_{46}	b_{54}	b_{62}
b_7	b_{15}	b_{23}	b_{31}	b_{39}	b_{47}	b_{55}	b_{63}
b_8	b_{16}	b_{24}	b_{32}	b_{40}	b_{48}	b_{56}	b_{64}

(b)

b_1	b_2	b_3	b_4	b_5	b_6	b_7	b_8
b_9	b_{10}	b_{11}	b_{12}	b_{13}	b_{14}	b_{15}	b_{16}
b_{17}	b_{18}	b_{19}	b_{20}	b_{21}	b_{22}	b_{23}	b_{24}
b_{25}	b_{26}	b_{27}	b_{28}	b_{29}	b_{30}	b_{31}	b_{32}
b_{33}	b_{34}	b_{35}	b_{36}	b_{37}	b_{38}	b_{39}	b_{40}
b_{41}	b_{42}	b_{43}	b_{44}	b_{45}	b_{46}	b_{47}	b_{48}
b_{49}	b_{50}	b_{51}	b_{52}	b_{53}	b_{54}	b_{55}	b_{56}
b_{57}	b_{58}	b_{59}	b_{60}	b_{61}	b_{62}	b_{63}	b_{64}

(c)

Figure 3. Block interleaving of an 8×8 matrix. The 8×8 matrix. (b) Block interleaving of the matrix. (c) Effect of error bursts after de-interleaving.

b_1	b_2	b_3	b_4	b_5	b_6	b_7	b_8
b_9	b_{10}	b_{11}	b_{12}	b_{13}	b_{14}	b_{15}	b_{16}
b_{17}	b_{18}	b_{19}	b_{20}	b_{21}	b_{22}	b_{23}	b_{24}
b_{25}	b_{26}	b_{27}	b_{28}	b_{29}	b_{30}	b_{31}	b_{32}
b_{33}	b_{34}	b_{35}	b_{36}	b_{37}	b_{38}	b_{39}	b_{40}
b_{41}	b_{42}	b_{43}	b_{44}	b_{45}	b_{46}	b_{47}	b_{48}
b_{49}	b_{50}	b_{51}	b_{52}	b_{53}	b_{54}	b_{55}	b_{56}
b_{57}	b_{58}	b_{59}	b_{60}	b_{61}	b_{62}	b_{63}	b_{64}

(a)

b_{31}	b_{23}	b_{15}	b_7	b_{32}	b_{24}	b_{16}	b_8
b_{63}	b_{55}	b_{47}	b_{39}	b_{64}	b_{56}	b_{48}	b_{40}
b_{11}	b_3	b_{12}	b_4	b_{13}	b_5	b_{14}	b_6
b_{27}	b_{19}	b_{28}	b_{20}	b_{29}	b_{21}	b_{30}	b_{20}
b_{43}	b_{35}	b_{44}	b_{36}	b_{45}	b_{37}	b_{46}	b_{38}
b_{59}	b_{51}	b_{60}	b_{52}	b_{61}	b_{53}	b_{62}	b_{54}
b_{25}	b_{17}	b_9	b_1	b_{26}	b_{18}	b_{10}	b_2
b_{57}	b_{49}	b_{41}	b_{33}	b_{58}	b_{50}	b_{42}	b_{34}

(b)

b_1	b_2	b_3	b_4	b_5	b_6	b_7	b_8
b_9	b_{10}	b_{11}	b_{12}	b_{13}	b_{14}	b_{15}	b_{16}
b_{17}	b_{18}	b_{19}	b_{20}	b_{21}	b_{22}	b_{23}	b_{24}
b_{25}	b_{26}	b_{27}	b_{28}	b_{29}	b_{30}	b_{31}	b_{32}
b_{33}	b_{34}	b_{35}	b_{36}	b_{37}	b_{38}	b_{39}	b_{40}
b_{41}	b_{42}	b_{43}	b_{44}	b_{45}	b_{46}	b_{47}	b_{48}
b_{49}	b_{50}	b_{51}	b_{52}	b_{53}	b_{54}	b_{55}	b_{56}
b_{57}	b_{58}	b_{59}	b_{60}	b_{61}	b_{62}	b_{63}	b_{64}

(c)

Figure 4. Chaotic interleaving of an 8×8 matrix. The 8×8 matrix divided into rectangles (Shaded bits are bits affected by error bursts). (b) Chaotic interleaving of the matrix. (c) Effect of error bursts after de-interleaving.

5. Cooperative WSN

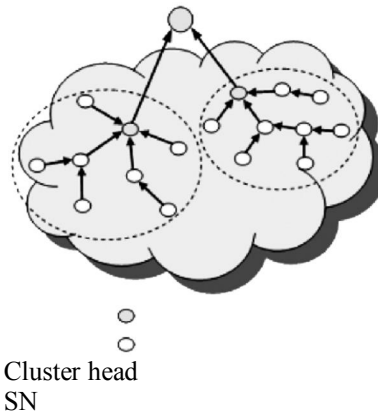


Figure 5. Multihop clustering architecture

The idea of cooperation intra-nodes of the WSN, shown in figure 5, contents aims to realize the

event confirmation and the power efficiency also. With the future of WSN and the manufacturing of microelectronics products, the mobility of sensing station won't be optional or imaginary. So, with supposing that the WSN in some particular application has some fixed sensing station and another group of mobile monitoring stations. The presented scenario here is based on the unique secret key of the interleaver chaotic based technique. Using this key, the nodes (get to know) can be known to other nodes, it may call it to confirm or neglect specific phenomenon or event. The mobility of some nodes leads to decreasing the need of tremendous number of nodes to cover specific service area. The secret key can be periodically changed by the controller or through defined algorithm within the sensing stations in the same service area. To confirm or deny a particular phenomenon or event, the mobile SN is proposed [41]. Figure 5 shows the deployment scenario of WSN sensing station with the cooperative link between the sensing stations. In the figure, it supposes that every cluster from the two cluster of SN has one unique secret key. It is used by the SNs to share the captured events and exchange the data among them [49].

4. Objective Quality Metrics

In this section, the different metrics are devoted to evaluate the presented scenarios for WSN performance with image transmission. The transmitted image over the mobile communication channel is very sensitive to the noise more than the fixed channel. The metrics are various to measure the received image samples quality and the reliability of the link also through the Bit Error Rate (BER) and the Number of Lost packets (NLP). First metric is the Peak Signal to Noise ratio (PSNR), it is utilized to measure the quality of received image samples. The PSNR of the received images is used as an evaluation metric in this paper. The Mean Square Error (MSE) is the cumulative squared error between the received image and the original image. The mathematical formula for MSE is given in Eq. (2) [42].

$$MSE = \frac{1}{MN} \sum_{y=1}^M \sum_{x=1}^N [I(x,y) - I'(x,y)]^2 \quad (2)$$

$$PSNR = 20 \times \log_{10} (255 / \sqrt{MSE}) \quad (3)$$

where $I(x,y)$ is the original image, $I'(x,y)$ is the received image, and M, N are the image dimensions. The higher PSNR is good that means the SNR is higher. Also, the case of lower MSE means lesser error, from Eqs. (2-3) there is the inverse relation between the MSE and PSNR. The best technique is having a lower MSE and higher

PSNR [43].

The second metric is used in this paper is measuring the degree of the correlation between the original and received images as given in Eq. (4) for different cases of our simulation [44].

$$C_r = \text{corr}(I(x,y), I'(x,y)) \quad (4)$$

C_r is correlation coefficient, $C_r = 1$ in the case of perfect correlation. As it approaches zero there is less of a relation, which means closer to uncorrelated.

The number of lost packet percentage is the metric of wireless channel reliability. The reliability of the link can be defined by the difference between the successes and corrected received packets and the total transmitted packets from the SN to the sink. The reliability R is given by the percentage of the sent packets that arrive correctly at the sink node and it may be evaluated from Eq. 5-9 as:

$$R = \frac{P_C}{P_S} \quad (5)$$

$$P_C = P_S - P_E \quad (6)$$

$$R = \frac{P_S - P_E}{P_S} \quad (7)$$

P_C is the number of corrected packets, P_S is

the total of transmitted packets. P_E is the number of dropped packets.

The NLP percentage is the number of failed packet to the total number of transmitted packets from the node to the sink [45].

$$NLP\% = \frac{P_S - P_C}{P_S} \times 100 \quad (8)$$

So, with lower NLP means higher reliability of link. It means also, lower retransmission request times and power efficient link.

BER=No. of bit error/length of packet*N iteration

PER=No. of dropped packets/Total Send packet, the dropped packet ratio to the total send packets.

NLP=Total send packet - success received packets.

$$NLP\% = NLP / \text{Total} * 100 \quad (9)$$

Also, from the comparison purpose at different SNRs, the number of lost frames is studied with the channel SNR. In our work, MATLAB was used for carrying out the simulation experiments of different cases. The simulation results have been gotten by transmission of the image over different SNR values [46].

6. Simulation Results

In this section, the computer simulation results are presented. A correlated Rayleigh fading channel is used. The channel model utilized is the Jakes model [47, 48]. The assumed mobile ZigBee device velocity is 10 miles/hour, and the carrier frequency is 2.46 GHz. The Doppler spread is 36.6 Hz. Figure 6 gives the original Cameraman image used in the experiments. The computer simulation section contains three categories of experimental simulations.



Figure 6. Original Cameraman image.

6.1 Mobility Effects on The Image Transmission

This section is devoted for studying the effects of the mobility of the ZigBee device (V_c) on the transmitted packets and the received images. The ZigBee employs the 16-bit Cyclic Redundancy Check (CRC) for error detecting scheme. In this computer experiment, the V_c is 1, 10, 20, 30, and 40 miles/hour. Figures 7 and 8 give the received images at SNR= 10 and 20 dB, respectively. Figure 9 shows the PSNR variation of the received images sample with the channel SNR.

Figure 10 gives the NLP variation with the channel SNR. It is clear that with increasing the V_c of the terminal, the NLP is increased.

The mobility effects on the error performance of the transmitted bit stream from SN to the sink using ZigBee technology through BER variation with the channel SNR is shown in Figure 11. It is clear that with increasing the V_c of the terminal, the error performance of the system is degraded.

6.2 Interleaving Techniques for a Correlated-Fading Channel.

In this section, different scenarios are employed for the image transmission over the ZigBee network. The image binary sequence to be transmitted is fragmented into packets. The PSNR of the received images is used as an evaluation metric in this paper.

In the first experiment, the Cameraman image is transmitted over a correlated-fading channel with Signal-to-Noise Ratio (SNR) = 10 dB. Different

scenarios of no interleaving, block interleaving, convolutional interleaving and chaotic interleaving are considered for comparison. The results of this experiment are shown in Figure 12. From these results, it is clear that the effects of all interleaving schemes is approximately equal at low SNR values.

Another experiment is repeated with SNR = 30 dB and the results are shown in Figure 13. From these results, we notice that the chaotic interleaver outperforms the other interleavers at moderate and high SNRs.

For the comparison purpose, the variation of the PSNR of the received image, the number of lost packets or frames and the Bit Error Rate (BER) with the channel SNR are studied and the results are shown in Figures 14 and 15. From these results, it is clear the chaotic interleaver enhancement begins at medium SNR values.



a- PSNR=22.7 dB



b- PSNR=21.7 dB



c- PSNR=21.6 dB



d- PSNR=21.5 dB



e- PSNR=21.3 dB

Figure 7. Received Cameraman image over a correlated fading channel at SNR =10 dB with (a) PSNR=22.7 dB, (b) PSNR=21.7 dB, (c) PSNR=21.6 dB, (d) PSNR=21.5dB, and (e) PSNR=21.3dB.

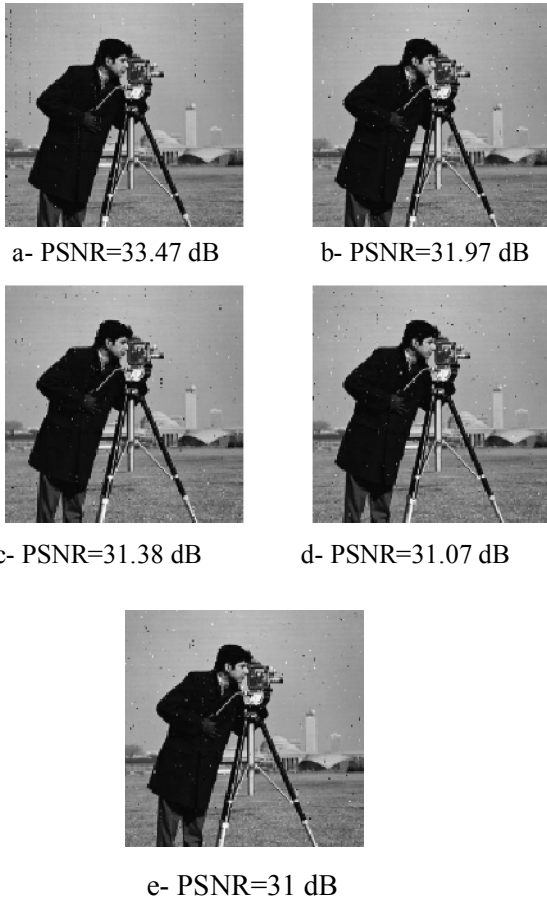


Figure 8. Received Cameraman image over a correlated fading channel at SNR =20 dB with (a) PSNR=33.47 dB, (b) PSNR=31.97 dB, (c) PSNR=31.38 dB, (d) PSNR=31.07 dB, and (e) PSNR=31.0 dB.

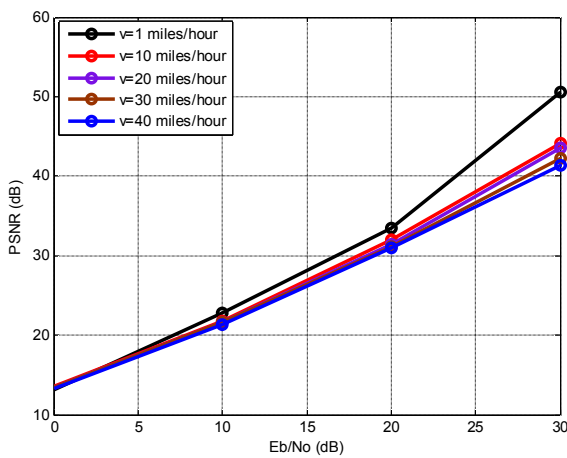


Figure 9. PSNR vs. SNR for the received Cameraman image over the ZigBee standard with the different V_c .

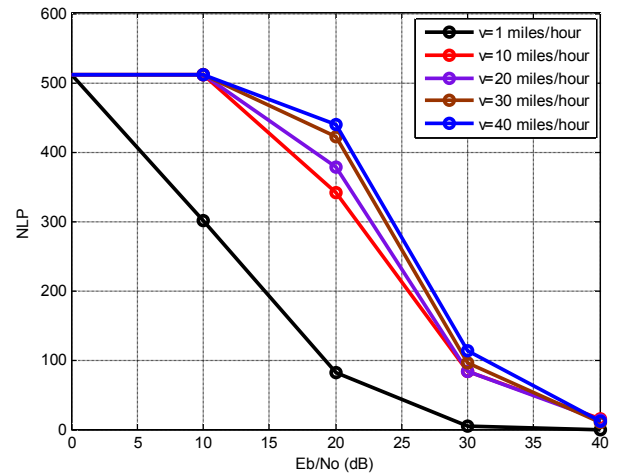


Figure 10. NLP vs. SNR for the received Cameraman image over the ZigBee standard with the different V_c .

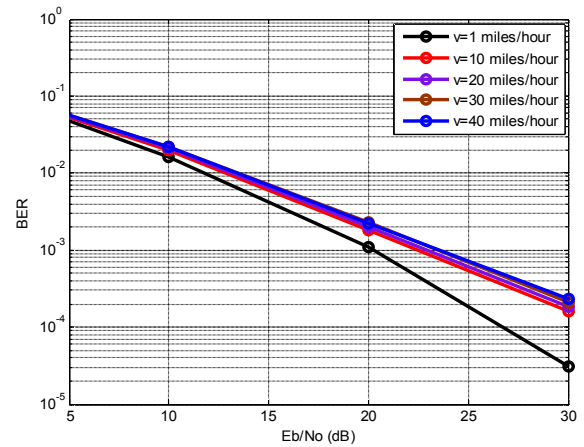
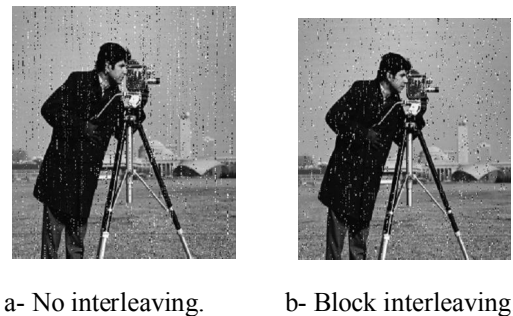
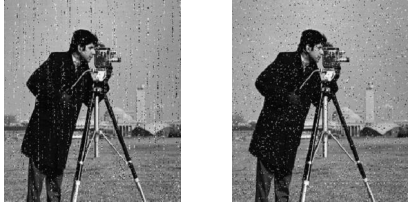


Figure 11. BER vs. SNR for the received Cameraman image over the ZigBee standard with the different V_c .





c- Convolutional interleaving d- Chaotic Interleaving
 Figure 12. Received Cameraman image over a correlated fading channel at SNR =10 dB with (a) PSNR=21.3 dB, (b) PSNR=21.4 dB, (c) PSNR=21.1 dB, and (d) PSNR=21.5 dB.

6.2 Constraint Length Effect

This section is devoted to investigate the effect of the constraint length K of the convolutional code on the image transmission process. The Cameraman image is transmitted over a correlated fading channel having SNR = 10 dB using convolutional coding only with code rate =1/2, and without interleaving. Constraint lengths of $K=3, 5,$ and 7 are investigated. Simulation results for this section are shown in Figure 15. From these results, it is clear that the effect of the constraint length on the received image is marginal at SNR=10 dB. The variations of the PSNR of the received image with the channel SNR for different constraint lengths are shown in Figure 16. It is clear from that figure that a large constraint length gives better PSNR performance, especially at medium and high SNR values in the channel at the expense of an increased complexity.



a- No interleaving. b- Block interleaving.



c- Convolutional interleaving. d- Chaotic Interleaving.

Figure 13. Received Cameraman image over a correlated fading channel at SNR=30 dB with (a) PSNR=39.1 dB, (b) PSNR=41 dB, (c) PSNR=41.1 dB, and (d) PSNR=43.1 dB.

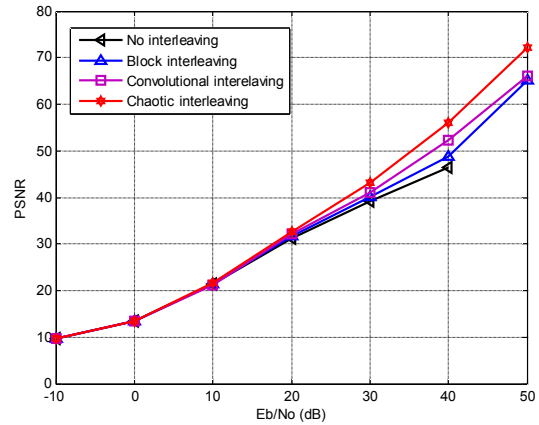


Figure 14. PSNR vs. SNR for the received Cameraman image over a correlated fading channel.



a- Code rate =1/2, K=3 b- Code rate =1/2, K=5.



c- Code rate =1/2, K=7.

Figure 15. Received Cameraman image over a correlated fading channel at SNR=10 dB using the convolutional code with code rate = 1/2 and different constraint lengths, (a) PSNR=23.12 dB, (b) PSNR=23.35 dB, and (c) PSNR=23.73 dB.

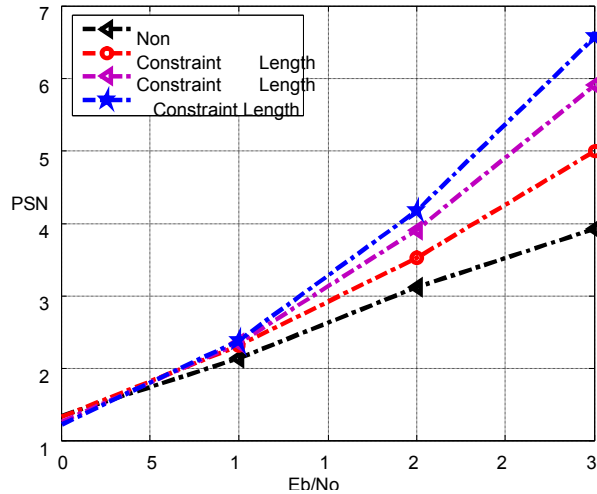


Figure 16. PSNR vs. SNR for the received Cameraman image over a correlated fading channel with different constraint lengths.

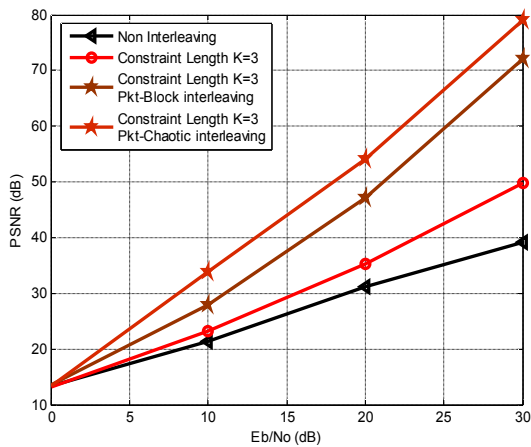


Figure 17. PSNR vs. SNR for the received Cameraman image over a correlated fading channel with different scenarios for image transmission.

6.3 Chaotic Interleaving on a Packet-by-Packet Basis

The proposed chaotic interleaver can be implemented on a packet-by-packet basis. Simulation experiments are carried out in this section to compare between four cases; no coding or interleaving, convolutional coding with code rate = 1/2 and K=3, convolutional coding with block interleaving on a packet-by-packet basis, and convolutional coding with chaotic interleaving on a packet-by-packet basis. The results of these experiments are shown in Figure 17.



a- No coding or interleaving b- Block interleaving



c- Chaotic interleaving

Figure 18. Received Cameraman image over a correlated fading channel at SNR=10 dB using the convolutional coding with code rate = 1/2 and K=3, (a) PSNR=23.12 dB, (b) PSNR=27.8dB, and (c) PSNR=33.85dB.

Some sample received images are shown in Figure 18. This figure reveals that the proposed chaotic interleaver on a packet-by-packet basis achieves the highest PSNR values with a convolutional code having K=3.

6.4 General Comparison

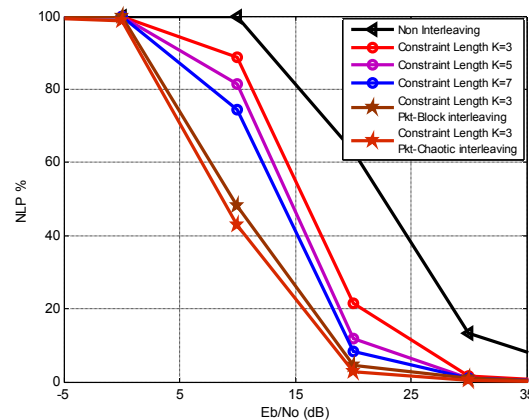


Figure 19. NLP % vs. SNR for the received Cameraman image over a correlated fading channel in the ZigBee network.

This section gives a comparison between the different Scenarios for image transmission over the ZigBee network based on the Number of Lost Packet (NLP %) and the PSNR. Figure 19 shows the variation of the NLP % with the channel SNR for the

Cameraman image transmission over a correlated fading channel for the different scenarios. This figure indicates the efficiency of the proposed chaotic interleaver. As shown in this figure, the chaotic interleaver on a packet-by-packet basis is effective at low SNR values for short constraint length convolutional encoders.

Figure 20 shows the variation of the PSNR with the channel SNR for the Cameraman image transmission over a correlated fading channel for the different scenarios. It is clear that the received images using the chaotic interleaver on a packet-by-packet basis have the highest PSNR values. The proposed technique with $K=3$ performs better than that with convolutional coding only with $K=7$. In fact, the complexity increases exponentially with K . This means that the complexity of the decoder with $K=7$ equals 16 times that of the decoder with $K=3$. So, with the proposed chaotic interleaving technique on a packet-by-packet basis, the performance is improved, while the complexity is reduced.

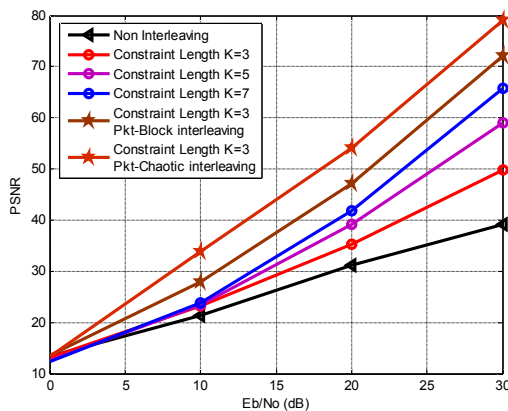


Figure 20. PSNR vs. SNR for the received Cameraman image over a correlated fading channel in the ZigBee network.

7. Conclusion

The ZigBee technology is WPAN network also, it widely used to implement the idea of WSN within many applications. The paper has presented a simple and efficient novel chaotic interleaver for the transmission of images over the WSN utilizing for this purpose the ZigBee network. Also, it has studied the performance of the proposed interleaver with convolutional codes having different constraint lengths. A comparison study between the proposed interleaver and the conventional interleavers has been presented. The computer simulation results have revealed the effectiveness of the proposed interleaver at medium and high SNR values. The results have also proved that the chaotic interleaver improves the

performance of the convolutional codes with short constraint lengths. It means the encoder with $K=3$ with the chaotic interleaver performs better than the encoder with $K=7$. In addition, the proposed scheme has the ability to enhance the security of the ZigBee network, because it permits the change of Skey from packet to packet. So, we can conclude that the proposed interleaving technique chaotic based scheme on a packet-by-packet basis is suitable for ZigBee communication with lower complexity. So, the presented scenarios discussed within essential issues of WSN the complexity and the reliability with the security challenges. The scenarios proven that the wireless link of WSN can be more reliable and secured with it, no need for more complex encoders in worst environment of transmission.

Acknowledgment

This work was funded by the Deanship of Scientific Research (DSR), King Abdulaziz University, Jeddah, under grant No.(829-011-D1434). The Authors, therefore, Acknowledge with thanks DSR technical and financial support.

Corresponding Author:

Prof. Ahmed A. Abouelfadl
Department of Electrical Engineering
Faculty of Engineering, Rabigh 21911
King Abdulaziz University, Saudi Arabia
E-mail: ahmed251056@yahoo.com

References

1. Akyildiz, W. Sankarasubramaniam, Y. Cayirci, A survey on sensor networks. *IEEE Commun. Mag.* 2002, (40), 102–114.
2. R. Verdone, D. Dardari, G. Mazzini and A. Conti, *Wireless Sensor and Actuator Networks*. Elsevier: London, UK, 2008.
3. Verdone, R. ,*Wireless Sensor Networks*. Proceedings of the 5th European Conference, Bologna, Italy, 2008.
4. Culler, D.; Estrin, D.; Srivastava, M., Overview of sensor networks. *IEEE Comput. Mag.* 2004, (37), 41–49.
5. V. Bhargava, D. Haccoun, R. Matyas, and P. Nuspl, *Digital Communications by Satellite*. New York: Wiley, 1981.
6. Emad N. Farag, Mohamed I Elmasry, *Mixed Signal VLSI Wireless Design Circuits and System*, 1st Edition, Kluwer Academic Publishers, 1999.
7. S. Lin and D. J. Costello, *Error Control Coding: Fundamentals and Applications*. Englewood Cliff, NJ: Prentice-Hall, 1983.
8. D. F. Yuan, Z. W. Li, A. Sui, and J. Luo, Performance of interleaved (2,1,7) convolutional codes in mobile image communication system. in *Proc. IEEE Wireless Communications and Networking Conference*

- (WCNC '00), (2), pp. 634–637, Chicago, Ill, USA, September 2000.
9. F. Chan and D. Haccoun, Adaptive Viterbi Decoding of Convolutional Codes over Memoryless Channels. *IEEE Transactions on Communications*, Vol.45, (11), November 1997.
 10. N. Benvenuto, L. Bettella, and R. Marchesani, Performance of the Viterbi Algorithm for Interleaved Convolutional Codes. *IEEE Transactions on Vehicular Technology*, Vol. 47, (3), August 1998.
 11. J. J. Kong and K. K. Parhi, Interleaved Convolutional Code and Its Viterbi Decoder Architecture. *EURASIP Journal on Applied Signal Processing* 2003,(13), 1328–1334.
 12. Elkhazin, K. Plataniotis, and Subbarayan Pasupathy, Irregular Convolutional Codes in Multiantenna Bit-Interleaved Coded Modulation Under Iterative Detection and Decoding. *IEEE Transactions on Vehicular Technology*, Vol. 59, (7), September 2010.
 13. Basagni, S.; Conti, M.; Giordano, S.; Stojmenovic, I. *Mobile Ad Hoc Networking*; Wiley: San Francisco, CA, USA, 2004.
 14. Tubaishat, M.; Madria, S. Sensor networks: an overview. *IEEE Potentials* 2003, (22), 20–30.
 15. Chiara Buratti, Andrea Conti, Davide Dardari and Roberto Verdone, An Overview on Wireless Sensor Networks Technology and Evolution. *Sensors* 2009, (9), 6869-6896.
 16. João H. Kleinschmidt, Walter C. Borelli, Marcelo E. Pellenz, An analytical model for energy efficiency of error control schemes in sensor networks. This full text paper was peer reviewed at the direction of IEEE Communications Society subject matter experts for publication in the ICC 2007 proceedings.
 17. J. Meer, M. Nijdam and M. Bijl, Adaptive error control in a wireless sensor network using packet importance valuation. *Hardware/software co-design*, Enschede, Netherlands, May 2003.
 18. J. H. Kleinschmidt, W. C. Borelli and M. E. Pellenz, Power efficient error control for Bluetooth-based sensor networks. *IEEE Local Computer Networks Conference*, Sydney, Australia, November 2005.
 19. W. Dargie and Christian Poellabauer, *Fundamental of Wireless Sensor Networks Theory and Practice*, A John Wiley and Sons, Ltd., Publication 2010.
 20. Kai, and P. Yong, Performance Study on ZigBee-Based Wireless Personal Area Networks for Real-Time Health monitoring. *ETRI Journal*, Volume 28, (4), Aug. 2006.
 21. Jin-Shyan Lee, Yu-Wei Su, and Chung-Chou Shen, A Comparative Study of Wireless Protocols: Bluetooth, UWB, ZigBee, and Wi-Fi. *The 33rd Annual Conference of the IEEE Industrial Electronics Society (IECON)*, Nov. 5-8, 2007, Taipei, Taiwan.
 22. W. Guo and M. Zhou, An emerging technology for improved building automation control. *IEEE International Conference on Systems, man and Cybernetics*, 2009. SMC 2009., pp.337-342, Oct. 2009.
 23. Sidhu, H. Singh, and A. Chhabra, Emerging Wireless Standards - WiFi, ZigBee and WiMAXs. *World Academy of Science, Engineering and Technology* (25) 2007.
 24. Xu, C., Soft decoding algorithm for RS-CC concatenated codes in WIMAX system. *Vehicular Technology Conference*, 2007.
 25. Gazi, O. and A. "Ozg"ur Yilmaz, Turbo product codes based on convolutional codes. *ETRI Journal*, Vol. 28, (4), August 2006.
 26. M. Kaiser, W. Fong, and M. Sikora, A Comparison of Decoding Latency for Block and Convolutional Codes. *Proceeding, ISCTA'09*, Ambleside, UK.
 27. J. Hagenauer, and L. Papke, Iterative Decoding of Binary Block and Convolutional Codes. *IEEE Transactions on Information Theory*, Vol. 42, (2), March 1996.
 28. S. H. Lee and E. K. Joo, The Effect of Block Interleaving in an LDPC-Turbo Concatenated Code. *ETRI Journal*, Volume 28, (5), October 2006.
 29. G. Pekhteryev, Z. Sahinoglu, P. Orlik, and G. Bhatti, Error Protection for Progressive Image Transmission Over Memoryless and Fading Channels. *IEEE Transactions on Communications*, Vol. 46, (12), Dec. 1998.
 30. S. Vafi, T. A. Wysocki, Application of convolutional interleavers in turbo codes with unequal error protection. *JTIT, Journal of Telecommunication and Information technology*, Jan. 2006.
 31. S. Shiyamala and Dr. V. Rajamani, A Novel Area Efficient Folded Modified Convolutional Interleaving Architecture for MAP Decoder. *International Journal of Computer Applications* Volume 9, (9), November 2010, 0975 – 8887.
 32. H. Zhang, L. Wang, Q. Yuan, H. Wang, L. Yu, A Chaotic Interleaver Used in Turbo Codes. *ICCCAS 2004, Int. Conference of Communications, Circuits, and Systems*.
 33. Z. Xuelan, L. Weiyan, and F. Guangzeng, Applying Chaotic Maps to Interleaving Scheme Design in BICM-ID. *Chinese Journal of Electronics* Vol.19, (3), July 2010.
 34. Y. Dong, L. Liu, C. Zhu, Y. Wang, Image Encryption Algorithm Based on Chaotic Mapping. *3rd IEEE International Conference on Computer Science and Information technology, ICCSIT*, 2010.
 35. M. Salleh, S. Ibrahim and I. F. Isnin, Enhanced chaotic image encryption algorithm based on Baker's map. *IEEE Conference on Circuits and Systems*, Vol.2, pp.508-511, 2003.
 36. N. Lemma, J. Aprea, W. Oomen, and L. V. de Kerkhof, A Temporal Domain Audio Watermarking Technique. *IEEE Transactions on Signal Processing*, Vol. 51, (4), pp. 1088-1097, 2003.
 37. W. Li, X. Xue, and P. Lu, Localized Audio Watermarking Technique Robust Against Time-Scale Modification. *IEEE Transactions on Multimedia*, Vol. 8, (1), pp. 60-69, 2006.
 38. G. Voyatzis and I. Pitas, Chaotic Watermarks for Embedding in the Spatial Digital Image

- Domain. Proc. IEEE Int. Conference Image Processing, Vol. 2, pp. 432-436, Oct. 1998.
39. R. Liu and T. Tan, An SVD-Based Watermarking Scheme for Protecting Rightful Ownership. IEEE Transactions On Multimedia, Vol. 4, (1), pp. 121-128, MARCH 2002.
 40. G. Pekhteryev, Z. Sahinoglu, P. Orlik, and G. Bhatti, Image Transmission over IEEE 802.15.4 and ZigBee Networks. IEEE ISCAS May 2005, Kobe Japan.
 41. W. C. Jakes, Microwave Mobile Communications. New York, John Wiley & SonsInc, Feb. 1975.
 42. Chiara Buratti, Andrea Conti , Davide Dardari and Roberto Verdone, An Overview on Wireless Sensor Networks Technology and Evolution. Sensors 2009, (9), 6869-6896.
 43. Akyildiz, I., Su, W., Sankarasubramaniam, Y. and Cayirci, E., A survey on sensor networks. IEEE Commun. Mag. 2002, (40), 102-114.
 44. Tubaishat, M.; Madria, S. Sensor networks: an overview. IEEE Potentials 2003, (22), 20-30.
 45. Hac, A. Wireless Sensor Network Designs. John Wiley & Sons Ltd: Etobicoke, Ontario, Canada, 2003. Sensors 2009, (9), 6894.
 46. Raghavendra, C.; Sivalingam, K.; Znati, T., Wireless Sensor Networks. Springer: New York, NY, USA, 2004.
 47. Sohrabi, K., Gao, J., Ailawadhi, V., and Pottie, G., Protocols for self-organization of a wireless sensor network. IEEE Personal Commun. 2000, (7), 16-27.
 48. Culler, D., Estrin, D., and Srivastava, M., Overview of sensor networks. IEEE Comput. 2004, (37), 41-49.
 49. João H. Kleinschmidt, Walter C. Borelli, Marcelo E. Pellenz, An analytical model for energy efficiency of error control schemes in sensor networks. IEEE Communications Society subject matter experts for publication in the ICC 2007 proceedings.
 50. Technology Digest, Wireless Sensor Network. Telecom Regulatory Authority of india, Issue 10, April 2012.

5/6/2014